'92 KACC 1992. 10. 19~21

POSITION ESTIMATION USING COMBINED VISION AND ACCELERATION MEASUREMENT

Yoonsu Nam

Stability and Control Lab., Agency for Defense Development

ABSTRACT

There are several potential error sources that can affect the estimation of the position of an object using combined vision and acceleration measurements. Two of the major sources, accelerometer dynamics and random noise in both sensor outputs, are considered. Using a second-order model, the errors introduced by the accelerometer dynamics are reduced by the smaller value of damping ratio and larger value of natural frequency. A Kalman filter approach was developed to minimize the influence of random errors on the position estimate. Experimental results for the end-point movement of a flexible beam confirmed the efficacy of the Kalman filter algorithm.

INTRODUCTION

Accurate, high bandwidth measurement of position is essential to quality performance of a feedback position control system. In many cases it is not convenient to make such measurements with direct contact sensors, for example, in the case of the end point of the robot. In these situations machine vision can be used. The sampling rate in machine vision is restricted by video image processing time, and the errors in such measurements may not be acceptable. The use of an inertial measurement between vision samples can be used to reduce both of these difficulties. The use of an accelerometer attached to the control object is used to supplement the vision measurements to arrive at a higher bandwidth and more accurate position estimator. Accelerometers are also not perfect in at least two ways. Accelerometers have limited bandwidth and there is noise in the accelerometer output.

The errors introduced by the accelerometer dynamics are considered using a second-order model [7]. In this analysis, the error magnitude caused by imperfect accelerometer dynamics is reduced by increases in the natural frequency and decreases in the damping ratio for frequencies well below the natural frequency. In the next section, a Kalman filter algorithm for minimizing the effects of random errors in both sensor outputs on the position estimate is developed. Finally, for an experimental verification, the end point displacement of a flexible beam is estimated by using a piezoresistive type accelerometer and landmark tracking system (LTS). The LTS is a grey-scale industrial vision system using pinhole imaging [1, 5].

APPLICATION OF KALMAN FILTER TO POSITION ESTIMATION

Consider now an one dimensional dynamic system in Fig. 1 used to estimate the position of an object based on the output of an accelerometer and a vision system. The state representation of such a dynamic system is

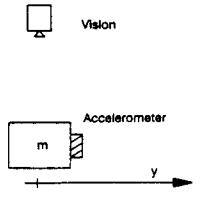

Fig. 1 One dimensional dynamic system

$$\dot{x} = \begin{bmatrix} 0 & 1 \\ 0 & 0 \end{bmatrix} x + \begin{bmatrix} 0 \\ 1 \end{bmatrix} (u + w) \\ = Ax + B(u + w) \tag{1}$$

with output equation,

$$z = \begin{bmatrix} 1 & 0 \end{bmatrix} x + v \\ = Hx + v \tag{2}$$

where

$x = [y\ \dot{y}]^T$

y = actual position

z = measured position

u = measured acceleration

w = error in acceleration measurement

v = error in position measurement

It will be assumed that the error is "white noise", which means that the subsequent analysis considers errors caused only by random effects, and not the effects of dynamics considered earlier, or any other systematic errors in the sensors.

If we assume T and T_v be the sample time intervals for the accelerometer and vision system respectively, where there is an integer N such that T_v= NT, then the system dynamics is changed to [3]

$$x_{k+1} = \begin{bmatrix} 1 & T \\ 0 & 1 \end{bmatrix} x_k + \begin{bmatrix} T^2/2 \\ T \end{bmatrix} (u_k + w_k) \\ = Fx_k + G(u_k + w_k) \tag{3}$$

where now x_k and x_{k+1} are the current and next state respectively. This sampling procedure is described in Fig. 2. Because a vision measurement is available only at every T_v second, the measurement equation is given as

$$z_{(k+1)N} = \begin{bmatrix} 1 & 0 \end{bmatrix} x_{(k+1)N} + v_{(k+1)N} \\ = Hx_{(k+1)N} + v_{(k+1)N} \tag{4}$$

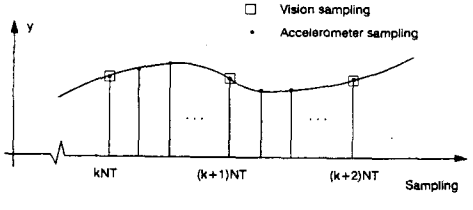

Fig.2 Sampling of a vision and accelerometer data

During the interval [kNT, (k+1)NT), during which time no vision measurement made, the estimate of state x, and error covariance P grows according to [4]

$$\hat{x}_{k+1} = F\hat{x}_k + Gu_k \\ P_{k+1} = FP_kF^T + GR_wG^T \tag{5}$$

where

$\hat{x}_k$ = estimate of the state at t = kT

$R_w = E\{ww^T\}$

$P_k = E\{(x_k - \hat{x}_k)(x_k - \hat{x}_k)^T\} = \begin{bmatrix} P_{yk} & P_{yvk} \\ P_{yvk} & P_{vk} \end{bmatrix}$

After some matrix manipulations, the relationship between the initial value of P_{kN} and the final value of $P^-_{(k+1)N}$ (at NT^-, or T_v^- ,i.e. error covariance matrix just before the vision measurement at t = (k + 1)NT) is given by

$$P^-_{y(k+1)N} = a_1R_w + P_{ykN} + 2NTP_{yvkN} + N^2T^2P_{vkN} \\ P^-_{yv(k+1)N} = a_2R_w + P_{yvkN} + NTP_{vkN} \\ P^-_{v(k+1)N} = a_3R_w + P_{vkN} \tag{6}$$

where

$$a_1 = N^3T^4/3 - NT^4/12 \\ a_2 = N^2T^3/2 \\ a_3 = NT^2$$

When a vision measurement is available, the estimate of state, is modified by the measurement update equation.

$$\hat{x}_{(k+1)N} = \hat{x}^-_{(k+1)N} + L_{(k+1)N}\{z_{(k+1)N} - H\hat{x}^-_{(k+1)N}\} \tag{7}$$

where

$$L_{(k+1)N} = P^-_{(k+1)N}H^T\{HP^-_{(k+1)N}H^T + R_v\}^{-1} \tag{8}$$

And error covariance matrix P is updated by

$$P_{(k+1)N} = \{I - L_{(k+1)N}H\}P^-_{(k+1)N} \tag{9}$$

where

$R_v = E\{vv^T\}$

$L_{(k+1)N}$ = Kalman filter gain

Because the above system is observable, the steady state Kalman filter gain and error covariance exist. Fig. 3 shows the typical variation of the error covariance of position, y, at steady state

versus time assuming that initially there is no error. Although the graph shows a continuous curve for P_y, a sample data system is being considered, so that only discrete values at intervals T are appropriate. The assumption of constant acceleration between samples is implicit. Because this assumption is not true, the random error in the acceleration measurement should be thought of as including this error as well as the sensor error itself.

In Fig. 3, P_{sy} is the maximum covariance of y in the steady state. It is this value which is of primary interest. Because of the assumption of no initial error in position estimation, P_{sy} starts from zero value, and grows according to Eq. (5). When the vision data is available, P_{sy} is decreased by the measurement update, i.e. Eq. (9). In steady state, this decrease must be equal to the increase given by Eq. (5). It is shown that the value of P_{sy} obeys [7]

$$A^2/(A+1) - N(A+2)\sqrt{NB/(A+1)} + B(2N^3+N)/12 = 0 \quad (10)$$

where

$$A = P_{sy}/R_v$$

$$B = T^4 R_w/R_v$$

Notice that A is normalized variance in the maximum error of the position estimation. If A is less than one, the system always has an expected error variance less than that of the vision system at the instant of the measurement. A can be greater than one because the maximum error occurs just BEFORE vision measurement. Fig. 4 is a design graph that relates A and B over a large range of possible values.

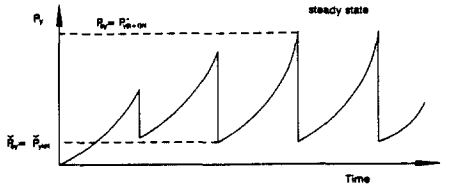

Fig. 3 Position error covariance vs. time, P(0)= 0

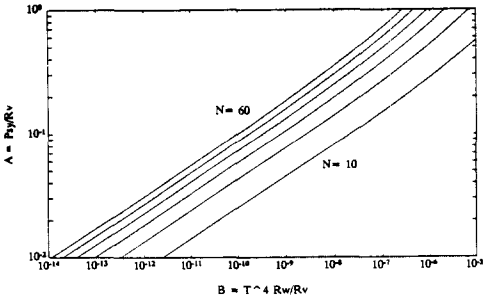

Fig. 4 Design reference plot of N, T, R_v and R_w

EXPERIMENT

Experiments on the estimation of the velocity and displacement of the flexible beam end point were made by combining an accelerometer and machine vision. By integrating the signal from the accelerometer attached to the beam end point, the velocity and position of the end point can be estimated. These estimated velocity and position data are corrected by vision data using the Kalman filter. To determine the Kalman filter gains, the noise levels of the accelerometer output signal and vision system data were measured.

Experimental devices

Fig. 5 shows the schematic diagram of the experimental setup. The flexible beam, which has the length of 28.5 inches, the thickness of 1/8 inches, and the width of 1.5 inches, is made of aluminum. A linear moving coil actuator, which is composed of a coil and permanent magnet (proof mass), was mounted on the top of the beam. This coil was fixed on the beam so that the generated magnetic force could be transferred to an end point of a beam directly, and permanent magnet was attached through a flexure spring to the beam.

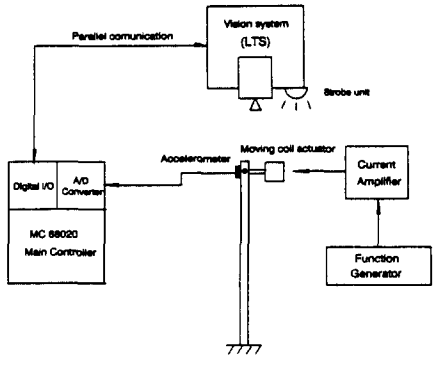

Fig. 5 Experimental setup

A piezoresistive type accelerometer, the model number of 3026-05-S manufactured from ICSensors [2], was attached at the end point of the beam. The accelerometer output signal was connected to a 32-bit MC68020 microprocessor [6] through an A/D converter. The main function of the MC68020 was sampling of the acceleration and vision data, and executing the Kalman filter algorithm of Eq. (5) and (7).

A landmark tracking system (LTS) was used for measuring the end point displacement of a flexible beam. The LTS [1,5] consists of a grey level CCD, a microcomputer (MC68000), a strobe unit, and software for tracking retroreflective landmarks. The retroreflective landmark attached to the beam end point is illuminated by the strobe unit. Because the landmark is much brighter than the other objects in the field of view if properly illuminated, it is mapped as very distinct spot on CCD array. This resulting image is transferred to the video RAM and processed by MC68000 computer of the LTS to calculate the landmark position. This position data were fed into MC68020 (the main controller) via a parallel communication.

Experimental results

The sampling rate of the acceleration of a beam end point was 2 msec. At every 100 msec, vision data were sampled. The noise levels of the LTS and accelerometer were determined by taking standard deviations of data being collected from a stationary state of the flexible beam. From the experimental data of the noise levels in Table 1, and this sampling relation, the Kalman filter gains can be found by Eq. (8). The steady state Kalman filter gains are 0.8603 for the position, and 7.2671 for the velocity correction. The steady state Kalman filter gain for the position correction is close to 1, which means the accuracy of vision data is much better than that of an accelerometer.

Two kinds of experiment were made. One was the estimation of position and velocity of a beam end point for the free vibration motion of a beam, and the other was about forced vibration by the moving coil actuator. For the free vibration, a flexible beam was initially disturbed by hand. It was a large scale motion from +1 to -1 inches. For the forced vibration, the beam was excited by the moving coil actuator attached to the beam end point. The excitation signal, a sine wave, from a function generator was amplified through a current amplifier. The forced vibration motion was a small scale motion from +0.1 to -0.1 inches.

Fig. 6 and Fig. 7 show the estimated position, velocity and the sensed acceleration of a beam end point for a free vibration motion. The mark 'x' in Fig. 6 represents a vision data from the LTS. The sudden rises and drops in the position and velocity estimation signals were the results from a correction by the Kalman filter. The first natural frequency of this flexible beam, which is about 1.5 Hz, can be identified experimentally from the Fig. 7.

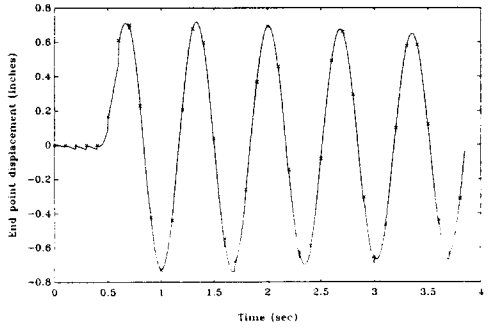

Fig. 6 Estimated position (Free vibration: 1.5 Hz)

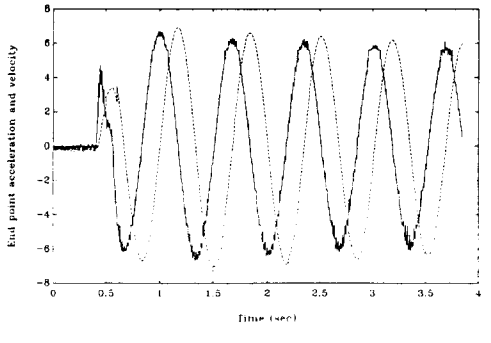

Fig. 7 Estimated velocity and sensed acceleration (Free vibration)

Table 1 Experimental data of the LTS and accelerometer

	Mean	Standard deviation
End point displacement/Pixel (inches)	4.4724×10^{-2}	x
Resolution of the LTS (inches)	x	1.0499×10^{-3}
Sensitivity of accelerometer (in/s^2)	1.0913×10^{2}	x
Resolution of accelerometer (in/s^2)	x	1.4437

Fig. 8 and Fig. 9 show the estimated signals for the forced vibration of about 2 Hz. Because of a small magnitude of acceleration, the noise in acceleration was seen clearly in Fig. 9. Even for this noisy acceleration signal, Fig. 8 shows that the position estimation by the Kalman filtering works well in recovering the movement of a beam end point. Because the frequency of this forced excitation (2 Hz) was close to the first natural frequency (1.5 Hz) of the flexible beam, the beat phenomenon could be occurred. The variation of the peak values in Fig. 8 and Fig. 9 is the result from the composition of a transient response, mainly by the first mode of the beam vibration, and a forced response.

For a high frequency excitation above 10 Hz, the steady state response magnitude of the end point displacement was much smaller than that of the transient response. To see the steady state response only, all the data were collected after 30 seconds from the instance of starting a forced vibration.

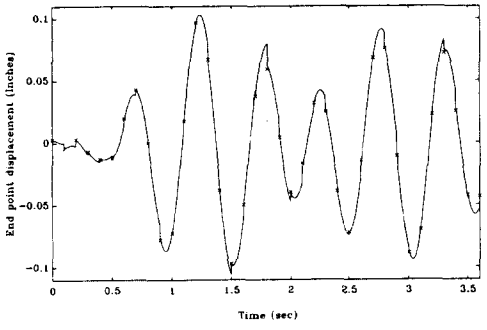

Fig. 8 Estimated position (Forced vibration: 2 Hz)

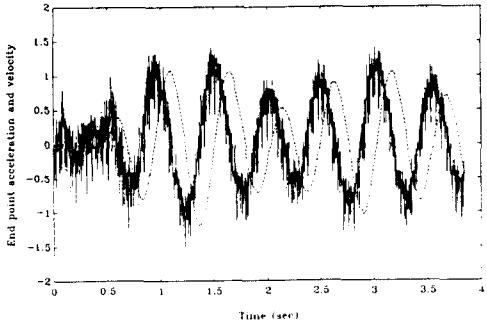

Fig. 9 Estimated velocity and sensed acceleration (2 Hz)

Fig. 10 and Fig. 11 are the estimated signals at steady state, when a flexible beam is excited by about 14 Hz sine wave signal. When the forced signal frequency is above 5 Hz, the vision sensor, which has a bandwidth of 10 Hz, can not recover the movement of a beam end point by the sampling theorem. As can be seen from Fig. 10, the measurement by a vision system does not have a 14 Hz signal. But, the estimated position shows clearly this frequency. Fig. 12 and Fig. 13 show the estimated signals at steady state for the input frequency of about 28 Hz. In Fig. 11 and Fig. 13, the acceleration signal is shifted intentionally for a clear display. Because the flexible beam is very lightly damped, the position estimation signals in Fig. 10 and Fig. 12 still have the transient response, even after 30 seconds from the initiation of a forced vibration.

The performance of the Kalman filtering for this combination of an accelerometer and vision system can be found by Eq. (10). By substituting the sampling rate of accelerometer, the covariance of an accelerometer noise and vision measurement noise, the non-dimensional parameter, B, can be calculated. The corresponding value of A, which is the ratio of the error covariance of estimated position to the covariance of a vision measurement noise, is 6.1599. Hence, the magnitude of error in the position estimation is 2.4819 times worse than the accuracy of the vision measurement. By using a better accelerometer, this error magnitude can be reduced to the order smaller than the accuracy of the vision system.

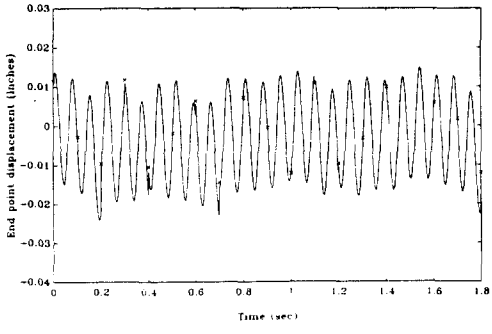

Fig. 10 Estimated position (Forced vibration: 14 Hz)

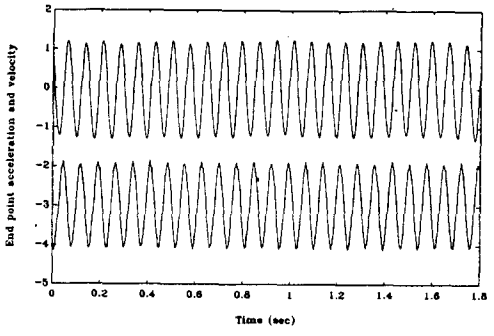

Fig. 11 Estimated velocity and sensed acceleration (14 Hz)

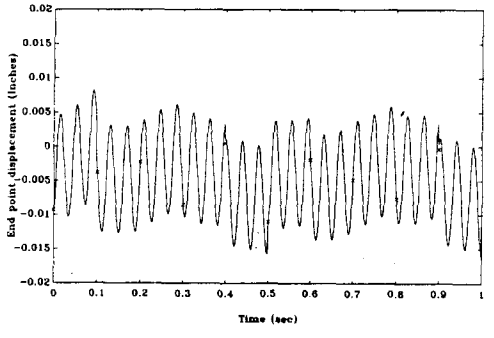

Fig. 12 Estimated position (Forced vibration: 28 Hz)

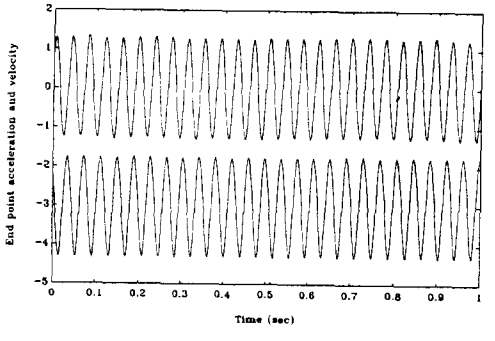

Fig. 13 Estimated velocity and sensed acceleration (28 Hz)

CONCLUSION

Errors due to accelerometer dynamics are minimized by smaller value of damping ratios and larger values of natural frequency provided that the natural frequency of the accelerometer is well above all significant frequencies in the motion being made.

A discrete Kalman filter to minimize the effects of noise in sensed acceleration and position was designed. A design equation relating the noises in the two measurements and error in the position estimate was derived. The position estimator using accelerometer and vision measurement showed good experimental results in recovering the movement of an object between each vision measurement even at a high frequency beyond the bandwidth of a vision measurement.

REFERENCES

1. Lee, E.H and Dickerson, S.L., "Pinhole imaging for industrial vision system", Symposium on Monitoring and Control for Manufacturing Processing, 1990 ASME WAM
2. Technical note TN-008 from ICSENSORS
3. Franklin, G.F and Powell, J.D., "Digital control of dynamic systems", Addison-Wesley Publishing Co., 1980
4. Gelb, A., "Applied optimal estimation", The M.I.T. Press, 1974
5. Dickerson, S.L. and Lee, E.H. and Lee, D. and Single, T, "Final report on Landmark tracking System for AS/RS", Material Handling Research Center, G.I.T., Feb. 1990
6. MVME 133 VMEmodule 32 bit Monoboard Microcomputer User's Manual, Motorola Inc., 1st Ed., 1986
7. Nam, Y.S., "Momentum Management for the End Point Control of a Flexible Manipulator", Ph.D Thesis, Georgia Tech., Mechanical Eng., 1991